

# Correlations between the proton temperature anisotropy and transverse high-frequency waves in the solar wind

Sofiane Bourouaine<sup>1</sup>, Eckart Marsch<sup>1</sup> and Fritz M. Neubauer<sup>2</sup>

bourouaine@mps.mpg.de

## ABSTRACT

Correlations are studied between the power density of transverse waves having frequencies between 0.01 and 1 normalized to the proton gyrofrequency in the plasma frame and the ratio of the perpendicular and parallel temperature of the protons. The wave power spectrum is evaluated from high-resolution 3D magnetic field vector components, and the ion temperatures are derived from the velocity distribution functions as measured in fast solar wind during the Helios-2 primary mission at radial distances from the Sun between 0.3 AU and 0.9 AU. From our statistical analysis, we obtain a striking correlation between the increases in the proton temperature ratio and enhancements in the wave power spectrum. Near the Sun the transverse part of the wave power is often found to be by more than an order of magnitude higher than its longitudinal counterpart. Also the measured ion temperature anisotropy appears to be limited by the theoretical threshold value for the ion-cyclotron instability. This suggests that high-frequency Alfvén-cyclotron waves regulate the proton temperature anisotropy.

## 1. Introduction

Several decades ago, the Helios in-situ measurements made in fast solar wind already showed that the proton temperature ratio,  $T_{\perp}/T_{\parallel}$ , in particular that of the core part studied here, was not unity but could reach high values of up to 3 at a distance of 0.3 AU from the Sun (Marsch *et al.* 1982), thus indicating strong local ion heating. With increasing heliocentric distance, this ratio tends to decrease, attaining values equal to unity or below only at 1 AU (Kasper *et al.* 2002).

---

<sup>1</sup>Max-Planck-Institut für Sonnensystemforschung, 37191 Katlenburg-Lindau, Germany

<sup>2</sup>Institut für Geophysik und Meteorologie, Universität zu Köln, Albertus-Magnus-Platz, Köln, 50923, Germany

Many theoreticians tried to explain the observed strong perpendicular ion heating, e.g., *Tu and Marsch* (2001); *Marsch and Tu* (2001) for the Helios results, *Cranmer et al.* (2009) and the many authors referenced therein for the fast solar wind. It is now widely believed that such kinetic features are in fact signatures of ion heating via ion-cyclotron resonance. However, it has also been questioned (e.g., *Cranmer et al.* 2001) whether ion-cyclotron waves do really exist near the Sun with sufficient power to provide the heating, or to enable the plateau formation in the proton velocity distribution functions (VDFs) observed in fast solar wind (*Tu and Marsch* 2002).

There is no general agreement yet on the physical process capable of explaining the heating of the ions and their temperature anisotropy. Recently, *Bale et al.* (2009) showed statistically that the gyroscale magnetic fluctuations at 1 AU are enhanced along the temperature anisotropy thresholds of the mirror, proton oblique firehose, and ion cyclotron instabilities which all seem to regulate the anisotropy. A possible wave generation scenario is that a nonlinear parallel cascade (via parametric decay) of low-frequency Alfvén waves may ultimately generate ion-cyclotron waves, whereby the protons and heavy ions can be heated perpendicularly via cyclotron-resonant wave absorption (*Araneda et al.* 2008, 2009; *Valentini et al.* 2009). In contrast to these models, it was argued that the energy density of the Alfvénic turbulence does not effectively cascade to the high-frequency parallel cyclotron waves but rather goes to low-frequency oblique kinetic Alfvén waves (with  $k_{\parallel} \ll k_{\perp}$ ). Then dissipation would still take place at the proton gyroscale, with  $k_{\perp} = \Omega_p/V_A$ , but via Landau damping acting mostly on electrons (*Howes et al.* 2008). Here  $\Omega_p = eB/(m_p c)$  is the proton gyrofrequency,  $B$  the magnetic field strength,  $e$  the elementary charge unit,  $c$  the vacuum speed of light,  $m_p$  the proton mass, and  $V_A = B/\sqrt{4\pi n_p m_p}$  the Alfvén speed involving the proton number density  $n_p$ . However, for ions Landau damping would lead to parallel heating, and hence in this way their temperature anisotropy in fast streams can not be explained.

Obviously, direct and more adequate wave observations are required in order to place new empirical constraints on the models and to limit the theoretical assumptions. In the present work benefiting from the high-resolution magnetic field data and the detailed proton VDFs obtained simultaneously by Helios 2, we will present such observations and establish a clear correlation between the proton temperature anisotropy and the power of high-frequency transverse waves.

## 2. Observations

The data set used in this study was provided by the Helios 2 probe during its primary mission, including the first perihelion passage in 1976 and covering distances from 0.3 to

0.9 AU from the Sun. Here we consider simultaneous measurements of the high-resolution 3D magnetic field vector components and the proton VDFs. These measurements have been made by two different instruments on board Helios 2, the magnetometer and the plasma experiment. The high-resolution magnetic field data were obtained with a sampling frequency that ranged up to values equal or higher than 4 Hz, corresponding to a Nyquist-frequency ranging up to values equal or higher than 2 Hz. This means that at all distances from the Sun, the field sampling rate is high enough to cover the resonances near the local proton cyclotron frequency,  $f_p = \Omega_p/(2\pi)$ .

The cadence of the plasma experiment for obtaining a VDF is typically 40.5 s, yielding about 90 VDFs per hour in the case of continuous measurements (for more details see, e.g., *Marsch et al.* 1982). This cadence is longer than the periods of the waves considered here. The Helios plasma experiment does not separate the energy distributions of the proton core (the major species) from the alpha particles and the proton beam. Since the mass-per-charge ratio,  $A/Z$ , of the alpha particles is 2, we expect that their VDFs should be clearly displaced from the maximum of the measured combined ion VDFs, and thus the core of a VDF represents the bulk protons. Since we are mainly interested in the core temperature anisotropy, we will only consider the innermost part of any VDF, where it is higher than 20 percent of its maximum value.

In Figure 1 we give a typical sample of the three components of the magnetic field vector and its magnitude, as obtained on day 105 in 1976 during a period that starts at time 00:22:20 and lasts for 3 minutes. At this time, the spacecraft was at a distance of 0.29 AU from the Sun. The magnetic field data (in nT) are given in solar-ecliptic coordinates and reveal the appearance of transverse (presumably Alfvén-cyclotron) waves with substantial amplitudes (note the constant magnitude field in Figure 1).

The left upper panel in Figure 2 displays the power spectrum density of the magnetic field turbulence measured during the time interval bound by two vertical solid lines in Figure 1. Note that there are peaks in the PSDs at a frequency of 1 Hz. These peaks are spurious and consequences of the small remaining errors in the zero-offsets and the spacecraft spin. However, in the case of the anisotropic VDF in the left top panel of Figure 2, there is a power enhancement below the Doppler-shifted proton cyclotron frequency,  $f'_p = f_p(1 + M_A)$ , involving the Alfvénic Mach number,  $M_A = V/V_A$ , of the solar wind with speed  $V$ . As we can not measure the wave vector  $\mathbf{k}$ , we assumed here the maximal possible Doppler shift for waves propagating outward from the Sun along the local magnetic field direction. A wave energy density enhancement near the cyclotron frequency has been found previously in other measurements, e.g. in spectra obtained at 1 AU (*Bale et al.* 2005).

In the right upper panel of Figure 2, we plot the corresponding proton VDFs measured

simultaneously during the same time interval when we studied the magnetic field fluctuations. Another example of a power spectrum, and the corresponding measured proton VDF, is plotted in the lower panel of Figure 2. The data of this example were obtained on the day 67 in 1976 at the time 21:37:12, when the spacecraft was at a distance of about 0.75 AU from the Sun. It is worth noting that these projected 2D VDFs are obtained from the 3D interpolation of the Helios plasma-experiment data. The VDFs appear to be gyrotropic, with their axes of the symmetry representing the direction of the background field (plotted as a solid straight line).

The wave power of the transversal component given in the upper panel (solid line) is about one order of magnitude higher than that of the longitudinal component (dashed line). Both components were computed with respect to the mean field vector defined by the average over a time interval of about 40 s. The transverse oscillations are composed essentially of incompressible waves. Unfortunately, due to the lack of corresponding ion bulk velocity fluctuations on that short time scale, it is not possible to confirm if these magnetic fluctuations are of Alfvénic nature. However, most likely they are (note the constant magnitude field in Figure 1), as Alfvén waves with periods larger than 40 s are observed extensively in fast solar wind (*Tu and Marsch 1995*).

Close inspection of the upper right panel of Figure 2 reveals the anisotropic shape of the core of the proton VDF. This characteristic form indicates preferential ion heating in the perpendicular direction with respect of the mean magnetic field. By comparing the two proton VDFs shown on the right panels of Figure 2, we can see a distinct difference between them. The one corresponding to higher wave power is more anisotropic than the proton VDF corresponding to lower power. We conclude from Figure 2 that perpendicular proton heating is strongly correlated with the power of transverse waves.

To provide more solid evidence for such a correlation between the proton temperature anisotropy and the enhanced transverse wave amplitude, we made a statistical analysis based on many measurements of both, high-resolution magnetic field vectors and proton VDFs, which were obtained at different locations from the sun. We selected 8 days of measurements in 1976, when the spacecraft was at heliocentric distances ranging between 0.29 and 0.95 AU from the Sun. Since our analysis only concerns the fast solar wind, we preferred those measurement where the spacecraft was crossing fast streaming plasma with a bulk speed higher than 600 km/s. Thus we selected several days, with DOY numbers 36, 46, 51, 61, 67, 76, 95 and 105, on which the spacecraft was, respectively, at the solar distances of 0.95, 0.90, 0.87, 0.79, 0.75, 0.65, 0.41 and 0.29 AU.

In this study, we used the temperature ratio,  $T_{\perp}/T_{\parallel}$ , as determined through computation of the parallel and perpendicular temperatures derived from the velocity moments of the

proton VDFs in 3D velocity space. Also, we dealt with the average wave power spectrum obtained by integration over the Doppler-shifted (indicated by a prime) frequency range,  $(0.01-1) f'$ . Therefore, the mean magnetic field is obtained by averaging the full magnetic field vector over a time interval of about  $10^2/f'$ .

Since the measurement cadence of the Helios plasma experiment is about 40 s, we have more than 2000 measurements per day, and thus more than 16000 measurements for 8 days. Unfortunately, because the spacecraft did not continuously encounter fast solar wind during the first perihelion passage, there is a distance gap in the selected data, i.e., we do not have adequate radial coverage between the distances 0.4 and 0.65 AU.

For the selected data set, we considered the mean values of the temperature ratio and total wave power. These mean values are obtained through averaging over each single hour of measurement time. Therefore, we have about 24 mean values of each measured quantity for a day, and thus totally for all selected data, we have about 192 average data points which are all plotted in Figure 3. Overall, the temperature ratio spans values between lower than 1 to a maximum of 3.5, and the total wave power ranges from low values of about  $0.5 \text{ nT}^2$  to high values of about  $300 \text{ nT}^2$ .

Notice that in Figure 3a an increase of the temperature ratio corresponds to an enhancement of wave power. However, as it is known from instability theory (*Gary* 1993), the temperature ratio tends to be limited by a threshold value at which the plasma becomes unstable. Furthermore, according to Figure 3b, the temperature ratio increases with increasing ratio of transversal to longitudinal total wave power. This latter ratio is mostly above 10 for temperature ratios above 1.5.

Considering the same data set, we now focus on the variation of the temperature ratio and the total wave-power versus different distances from the sun. The measured quantities given at each distance correspond to the mean values for one day of measurements, and therefore, we have eight points corresponding to the measurements made on days 36, 46, 51, 61, 67, 76, 95 and 105 in 1976 which are plotted as asterisks in Figure 4.

Both mean values, of the temperature ratio and total wave power, decrease from their higher values close to the Sun to lower values at the distance of 0.9 AU far from the Sun. The temperature ratio declines from a value of 3 at 0.3 AU to about 0.6 at 0.95 AU. Correspondingly, the total wave power drops from a value of about  $250 \text{ nT}^2$  at 0.3 AU to about  $2 \text{ nT}^2$  at 0.95 AU. The transversal component of the mean wave power near the Sun is almost 30 times higher than its longitudinal counterpart. Besides the total wave power, the ratio of its transversal-to-longitudinal components is also a decisive factor which seems to determine the observed variation of the temperature anisotropy in fast solar wind.

From the linear theory of the plasma waves instability (see e.g., *Gary* 1993) it is possible to obtain threshold values of the temperature anisotropy beyond which different wave modes will be excited, e.g., the ion-cyclotron, mirror or firehose modes. Based on the parallel plasma beta value (which ranges between about 0.1 and 0.6) we estimated in Figure 4 the typical threshold value of the temperature ratio for the ion-cyclotron (diamonds) and firehose (crosses) instabilities. It turns out that only at distances close to the Sun (0.3 and 0.4 AU), the value of the temperature ratio is near the threshold of the ion-cyclotron instability.

Apparently, due to the ion-cyclotron instability it seems not possible to produce closer the Sun higher temperature ratios than the actually measured ones. However, at distances greater than 0.5 AU from the Sun, the anisotropy threshold causing the ion-cyclotron instability reduces to lower values, mainly due to the radial increase of the plasma beta which for our data clearly stays below unity. Since the wave-power decreases with distance, the temperature ratios stay smaller than the threshold values for the ion-cyclotron instability (*Gary* 1993; *Tu and Marsch* 2002). But at distances beyond 0.9 AU, the temperature ratio reaches values smaller than unity, and then may hit the threshold for the firehose instability (*Kasper et al.* 2002).

### 3. Summary and discussion

As shown above, a strong core temperature anisotropy,  $T_{\perp}/T_{\parallel} > 1$ , appears in the proton VDFs in fast solar wind whenever the transverse magnetic field oscillations are enhanced. The temperature anisotropy, as well as the power of these (very likely) Alfvén-cyclotron waves ( $\omega \leq \Omega_p$ ), both are at their highest values at Helios perihelion distances near 0.3 AU. But at a farther distance of about 0.9 AU the temperature ratio has decreased to values equal to or below unity. Correspondingly, the wave power spectra decreased to much lower values, about two order of magnitudes less than at 0.3 AU.

It has been shown that the high temperature anisotropy is correlated with the enhanced transversal component of the waves in the frequency interval near but below the local proton gyrofrequency. Alfvén-cyclotron waves appear to have an important impact on proton heating and their resulting temperature anisotropy. We were not able from the data we had to discriminate a possible fast-magnetosonic component of these transverse waves. Their longitudinal component is likely related to the magnetosonic slow mode wave for our low-beta data.

Our findings support the notion that the ion heating process is connected with large-scale plasma turbulence. The idea that high-frequency ion-cyclotron waves are directly launched

at the Sun might not be a valid scenario. It seems more likely that these oscillations are generated and reabsorbed continuously in the expanding solar wind through an ongoing wave-particle cascade and regulated by temperature-anisotropy driven instabilities as studied, e.g., by *Tu and Marsch (2002)*; *Kasper et al. (2002)*; *Bale et al. (2009)* and/or the parametric decay as suggested by the simulations of *Araneda et al. (2008)*; *Valentini et al. (2009)*.

## REFERENCES

- Araneda, J. A., Y. Maneva, and E. Marsch (2009), Preferential Heating and Acceleration of  $\alpha$  Particles by Alfvén-Cyclotron Waves, *Phys. Rev. Lett.* *102*, 175001
- Araneda, J. A., E. Marsch, and A. F.-Viñas (2008), Proton Core Heating and Beam Formation via Parametrically Unstable Alfvén-Cyclotron Waves, *Phys. Rev. Lett.* *100*, 125003
- Bourouaine, s., E. Marsch, and C. Vocks (2008), On the Efficiency of Nonresonant Ion Heating by Coronal Alfvén Waves, *ApJ*, 684,L119L122, doi:10.1086/592243
- Bale, S. D., P. J. Kellogg, F. S. Mozer, T. S. Horbury, and H. Reme (2005), Measurement of the Electric Fluctuation Spectrum of Magnetohydrodynamic Turbulence, *Phys. Rev. Lett.* *94*, 215002
- Bale, S. D., J. C. Kasper, G. G. Howes, E. Quataert, C. Salem, and D. Sundkvist (2009), Magnetic Fluctuation Power Near Proton Temperature Anisotropy Instability Thresholds in the Solar Wind, *Phys. Rev. Lett.* *103*, 211101
- Cranmer, S. R. (2001), Ion cyclotron diffusion of velocity distributions in the extended solar corona, *J. Geophys. Res.* *106*, 24937
- Cranmer, S. R., W.H. Matthaeus, B.A. Breech, and J.C. Kasper (2009), Empirical constraints on proton and electron heating in the fast solar wind, *ApJ*. *702* 16041614
- Gary, P. S (1993), Gary, S. P.: *Theory of Space Plasma Microinstabilities*, Cambridge University Press, Cambridge, U.K.
- Howes, G. G. W. Dorland, S. C. Cowley, G. W. Hammett, E. Quataert, A. A. Schekochihin, and T. Tatsuno (2008), Kinetic Simulations of Magnetized Turbulence in Astrophysical Plasmas, *Phys. Rev. Lett.*, *100*, 065004
- Kasper, J. C., A. J. Lazarus, and S. P. Gary (2002), Wind/SWE observations of firehose constraint on solar wind proton temperature anisotropy, *GeoRL*. *17*, 170000

- Marsch, E., R. Schwenn, H. Rosenbauer, K. H. Muehlhaeuser, W. Pilipp, and F. M. Neubauer (1982), Solar wind protons - Three-dimensional velocity distributions and derived plasma parameters measured between 0.3 and 1 AU, *JGR.* *87*, 52
- Marsch, E., and C.-Y. Tu (2001), Heating and acceleration of coronal ions interacting with plasma waves through cyclotron and Landau resonance, *JGR.* *106*, 227
- Tu, C.-Y. and E. Marsch (2002), Anisotropy regulation and plateau formation through pitch angle diffusion of solar wind protons in resonance with cyclotron waves, *JGR.* *107*, 1249 doi:10.1029/2001JA000150
- Tu, C.-Y. and E. Marsch (1995), MHD structures, waves and turbulence in the solar wind: Observations and theories, *Space Science Rev.* *73*, 1
- Tu, C.-Y. and E. Marsch (2001), On cyclotron wave heating and acceleration of solar wind ions in the outer corona, *JGR.* *106*, 8233
- Valentini, F., P. Veltri, F. Califano, and A. Mangeney (2009), Cross-scale effects in solar wind turbulence, *Phys. Rev. Lett.* *102*, 225001

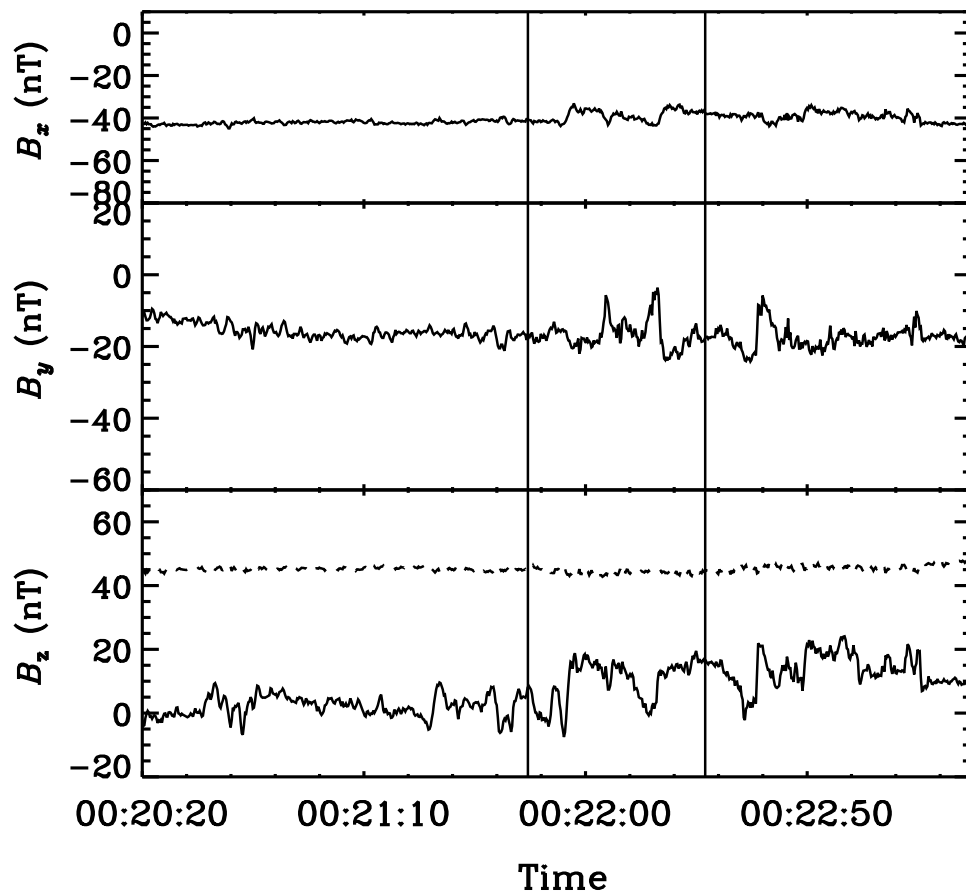


Fig. 1.— Example of magnetic field measurements versus time in seconds on day 105 in 1976 at 0.29 AU, whereby the field components and magnitude are given in solar-ecliptic coordinates, for which  $X$  points toward the Sun,  $Z$  towards the southern ecliptic pole, and  $Y$  completes the left-handed coordinate system. The magnitude of the full vector magnetic field (dashed line).

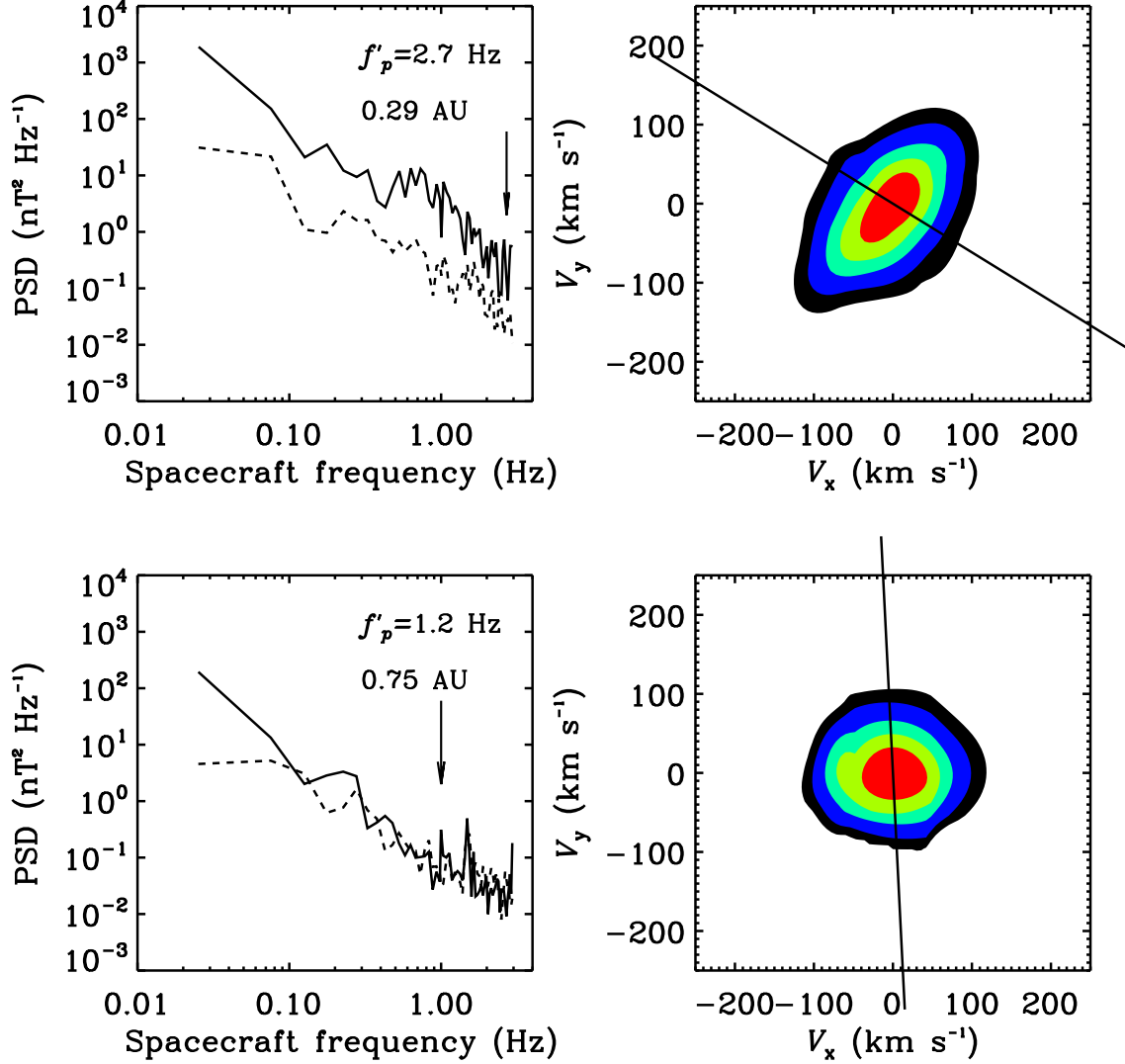


Fig. 2.— Top panels: The transversal (solid line) and longitudinal (dashed line) power spectrum (upper left panel) of the waves during the interval time shown between two solid lines in Fig.1, and the corresponding isodensity contours of the proton VDF (upper right panel) measured on day 105 in 1976 at 00:22:07. Bottom panels: Another example showing the wave power spectrum (lower left panel) during the time interval 21:36:50 and 21:37:32, and the corresponding proton VDF (lower right panel) measured on day 67 in 1976 at 21:37:12. The Doppler-shifted proton cyclotron frequency  $f'_p$  is marked by an arrow in the left panels.

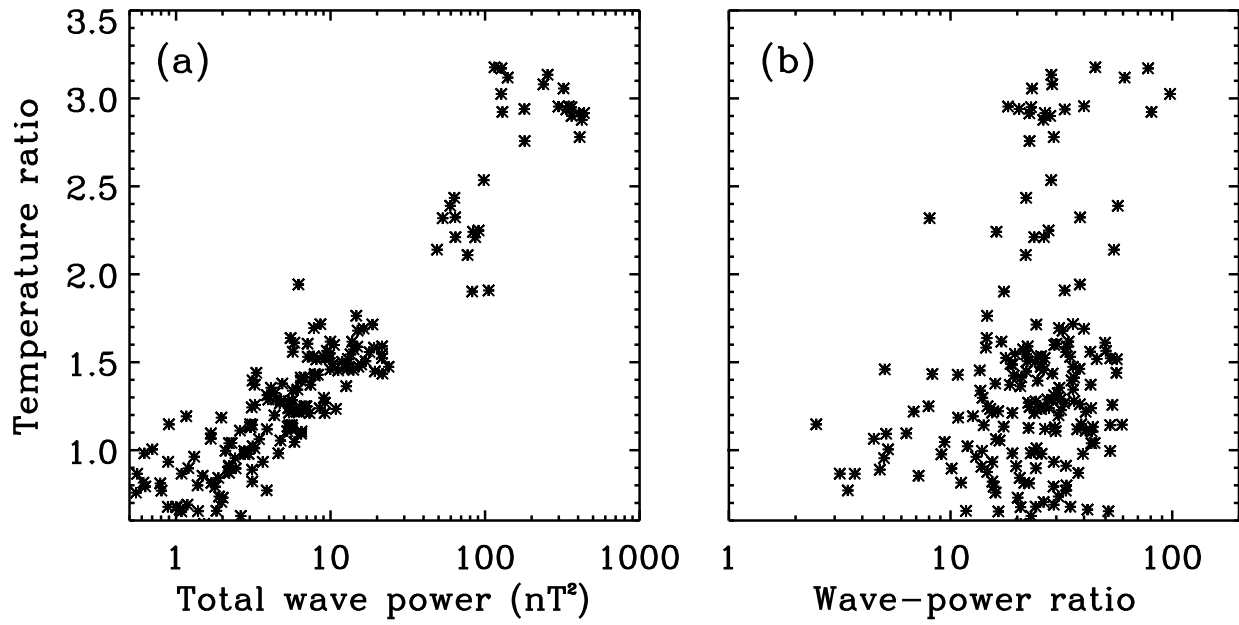


Fig. 3.— (a): Mean temperature ratio,  $T_{\perp}/T_{\parallel}$ , versus mean total wave-power (b): Mean temperature ratio,  $T_{\perp}/T_{\parallel}$ , versus the ratio of the transversal to the longitudinal wave power. The points correspond to the measurements made on days 36, 46, 51, 61, 67, 76, 95 and 105 in 1976.

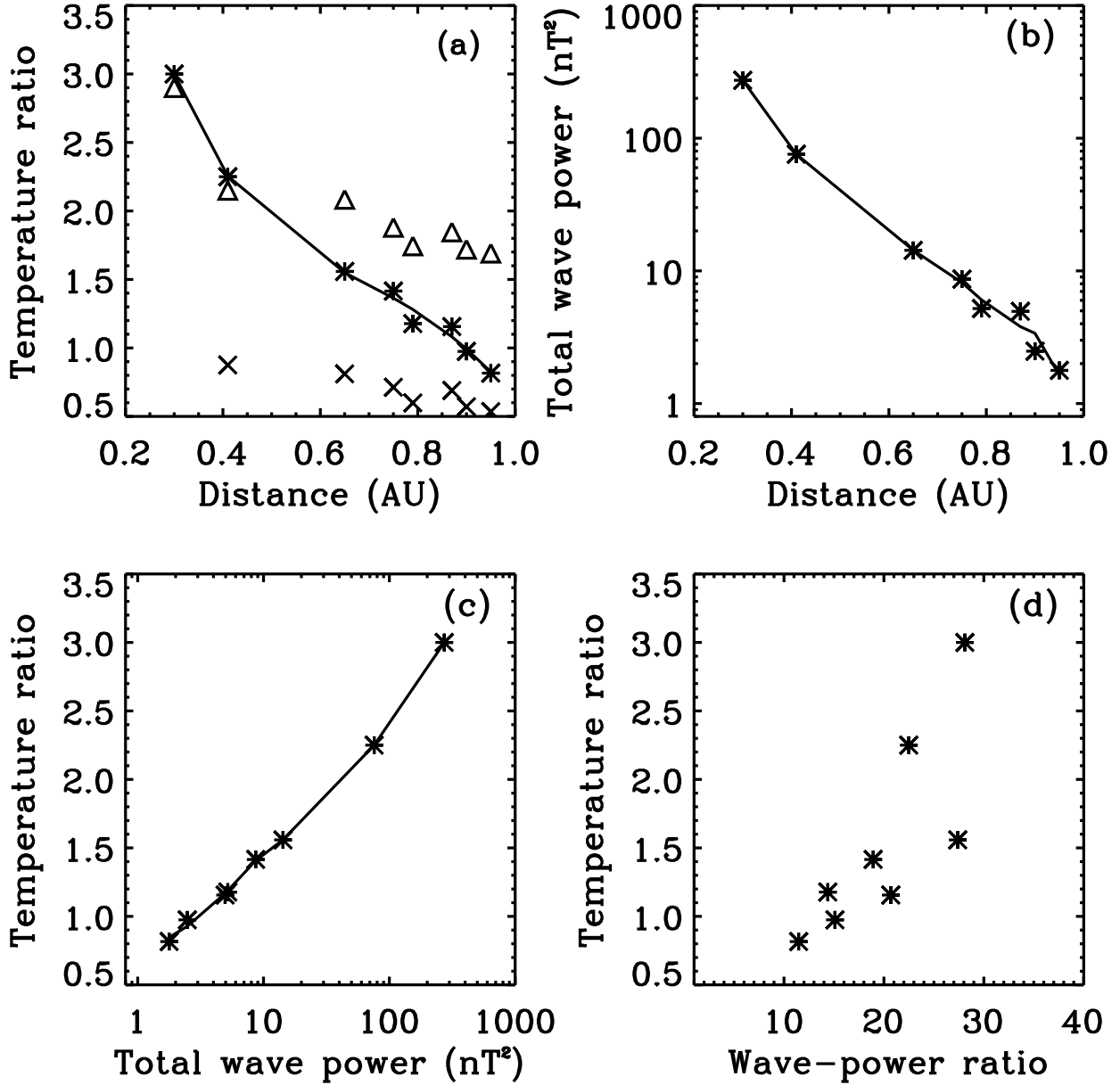


Fig. 4.— (a): Mean temperature ratio,  $T_{\perp}/T_{\parallel}$ , plotted versus distance from the Sun. A polynomial function was fitted to the data. The thresholds of the temperature-ratio for the ion-cyclotron instability (triangles), and for the firehose instability (crosses) are given for different distances from the sun. (b): Mean total wave power versus distance from the Sun, with a polynomial function fitted to the data. (c): Mean temperature ratio versus mean wave power, with a five-order polynomial function fitted to the data. (d): Mean temperature ratio plotted as a function of the ratio of the transversal to longitudinal wave power.